

An Improved Defocus Blur with Combined Local Binary Patterns and Nearest Neighbour Technique

A Jyothi Sravani, L V Narasimha Prasad

Computer Science and Engineering, Institute of Aeronautical Engineering, Dundigal, Hyderabad, India

Email: jyothisravani88@gmail.com; lvnprasad@yahoo.com

Abstract - Defocus blur is one of the phenomena in obtaining images using optical imaging systems. Blur parts mainly segment images into obscure or non-obscure regions. The existing research on defocus blur addresses the individual techniques based removal of blur. The present paper focuses on fused technique with a combination of local binary and nearest neighbor. In this the roughness metrics based on Local binary patterns (LBP) with a respective algorithm that isolates the clear-cut image regions. Based on the local binary patterns, roughness metric in local images mentions blurry regions. Applying these metrics in combination with image matting and multi scale inference achieves extreme levels of roughness. When LBP is combined with K-Nearest Neighbor (KNN) encompass a better outcome and also improves the efficiency of the segmentation with high-speed. This assures an improved treatment for blur images.

Keywords - Defocus blur, Optical Imaging Systems, LBP, Image Restoration, Image Segmentation, Identification, Object recognition, KNN.

I. INTRODUCTION

In images, Defocus blur is the outcome for an optical imaging system. Estimation of defocus blur plays a major role in computer graphic applications and in computer vision concepts including estimation of depth, assessment of image quality, image de-blurring and refocusing etc. Current image de-blurring methods consider that the blur is spatially fixed. Image regions can be specified by 3 types: blurred, sharp, and transitive. Three image features specify are taken into account, namely with color, texture, and shape. Defocus blur is large enough to be seen by human eyes. The purpose of segmenting defocus blur is to partition blurred and non-blurred regions by segmenting blur any further step will be easy. However, the current methods are unable to estimate the extent of blurriness. To solve this issue, new sharpness metric is introduced which is based on Local Binary Patterns, mainly used for pattern recognition.

Although, in some cases, separating blurred image as well as rough areas for an image can be difficult but the problem can be quickly resolved by image editing or replacing algorithms without affecting on rough areas, hence elements of photograph can be easily removed from inner regions. In this method the total image is divided into eight parts. Each part has some blur regions and sharpness values. The Image segmentation method involves for splitting a image into many components.

The goal of segmentation is to change the representation of an image into something more important, which makes examining easier. Normally Segmenting image is applied in background images and also for locating objects. More specifically, segmenting image is the process of assigning a label for every pixel in an image such that pixels with the same label share certain visual characteristics. Image

segmentation is a important signal processing tool that is widely employed in many applications including object detections, tracking objects etc. The fundamental procedure in segmenting image is thresholding which refers to the threshold value.

This method utilizes a Grayscale image for generating binary images. It ranges from (0-255), where 0 indicates the black color and 1 specifies the white color. Finally, gray scale images displays ground truth images with focus and defocus regions. In clustering one of the most fundamental learning algorithm is KNN can also referred as K-Nearest Neighbor. It is one of the simplest classification algorithms available for supervised learning and cluster the pixels which are near to intensity values and according to the number of pixels estimates both the distance metrics and the number of nearest neighbors. Extracting object is an important task in KNN classification. After extracting the image features each object classifies physical object elements. Categorization and partitioning are closely connected to each other but categorization can guide for partitioning. Classifying objects are based on the majority of its neighbors.

II. LITERATURE REVIEW

Measuring local sharpness via defocus blur segmentation has been a popular method for a while. Although there are multiple tasks in an image, the most important tasks that capture human attention are human quality and human roughness. Some computer applications simply specify sharpness value for a single image and the Kurtosis metric is defined as the statistical measure for distributing the peakedness used in terms of frequency domains for measuring sharpness [1]. Measurement of blur

is described in terms of spatial domain but the blur is perceptually visible along the edges and locates on the smooth effect of blur aims to measure the spread of edges [2]. Measuring sharpness is based on kurtosis based method which is the only possible method that relates with multivariate kurtosis which defines any univariate random variable with a Gaussian distribution. The value of a random variable compares with 3 determines the distribution as peaked which is relative to Gaussian Distribution [3].

Complex wavelet phases transform a domain that constitutes a pattern that is highly predictable in the scale space. The Generalization phase considers sharp image features for describing exact location of alignment across scales specify distinctive image features [4]. Both edge blurriness, distortion measures the detection of the recapturing process as a feature for a given image. While detecting edges recaptures fully characterized images by the Line Spread Function (LSF). The other approach for characterizing the blur is Point Spread Function (PSF). When PSF is not achieved LSF is achieved instead [5]. Most of these metrics measure each pixel around the edges and estimates by varying spatially with the amount of blur that refers to "Defocus Map". Defocus Map can be estimated in two ways: one way is for estimating the amount of blur at edges and another way is for measuring blur for the rest of the image [6].

The input image re-blurs using a Gaussian blur kernel estimates the blur near edge locations then calculates the ratio of input gradients and re-blurred images [7]. Approaches for Low depth of field image segments both edge-based and region-based images extracts every object with edges and regions. Alternatively, several methods like local variance coefficients and local variance image field utilize only high frequency components results errors in both focus and defocus regions. For reducing errors, a block-wise maximum a posteriori segment object of the image field generates smooth boundaries of adjacent defocused regions with focused regions. The concept of Depth of Field (DOF) in photography and its relationship with image segmentation refers sharply focused object [9]. A block wise MAP directly segments the field of low depth images. The estimations of local roughness areas depends upon the energy functions of the MAP formulation and are distinct from others. However, using a block-wise Gaussian Distribution estimates the average of local variance [10].

Measuring blur globally and locally is the main task in removing the spatially varying blur also enhances the visual quality information about the scene includes saliency and depth map [11].

Shi et al and Liu et al both suggested a method automatically detects blurred images for possible blurred regions. Detecting new blur and analyzing blurry regions together specifically designs blur features with spectral, gradient and color information. Both classifying the blur and detecting the blur are carried out in two ways: one way

is to detect blurred images involves combining 3 features with Gradient Histogram span and local power spectrum slope models the blur characteristics in different ways. On the other way, the blurred regions focused out among directional motion are distinguished by using another feature. The graphical representations classify with Kurtosis trains navae Bayes classifier in neighborhood regions [12]. The classification techniques are related to the alpha channel feature is used for classifying blur. The singular value decomposition features an image by the blurred region if it is greater than threshold value categorizes as non-blurred region [13].

Su et al. exploits a singular value decomposition method for identifying the blur in image detects thresholds in blurred regions. Vu et al. exploit local variation, local power spectrum slope for measuring both spatial and spectral domains. The local sharpness of an image estimates both spatial and spectral domains utilizes which are related to the image. Overall spatial variation and slope of the magnitude spectrum for each block are adjusted for visual perception combines with weighted geometric mean values results of spectral and spatial sharpness. All these sharpness yields a sharpness map that has greater values is considered with roughness regions [14]. Blur features with image decomposition and sparse representation directly estimate blur strength. Shi et al. suggested a sparse dictionary denotes dictionary atoms captures elementary information for natural images. In this, each image patch is considered as a dictionary jointly trains all image patches decomposes few atoms with non-zero elements [15]. However, the amount of blur estimates the opposite sign in the gradient direction calculates the distance between the second derivative [16].

Zhu et al. suggested a specific method for spatially varying defocus with Point Spread Function over an image reveals geometric information of the scene and estimates information for recovering an overall in-focused image. A PSF for a defocus blur with a single parameter scale indicates as an optimal blur for each pixel but some of the methods require a coded aperture filter for inserting a camera [17] and estimates MAP with local blur measures a small neighborhood region being blurred by a candidate blur kernel [18]. The darkness blur kernel of image blocks evaluates blind image deconvolution. Although, estimating re-blurring of the local blur kernels finds the degrees for image blocks [19]. Florent et al. proposed to degrade the deblurring process by some ways in that one way is for calculating the non uniform blur kernel combines local blur with global smoothness constraints, the other way is for recovering sharp images uses a deconvolution algorithm depends on sparse regularization [20]. The intention is only to separate inner regions from the defocus field. Moreover an individual blurry region expects little more response through rough regions; generally, all measurements vary in different cases. The next section represents our new metrics of roughness which is based on LBP. The scope for

response value in blur patches have less crossing point than rough regions have low contrast region but provides appropriate values.

III. LBP SEGMENTATION

LBP is strong in segmenting texture, face recognition, eliminating background, texture of 3D Surface etc.

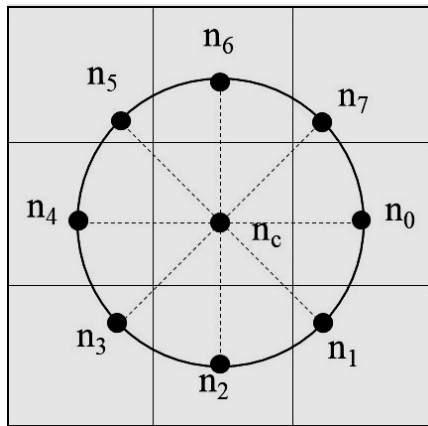


Fig. 1. 8 bit LBP

A LBP pixels in terms of x_c, y_c is defined as:

$$LBP_{P,R}(x_c, y_c) = \sum_{p=0}^{P-1} S(n_p - n_c) \times 2^p \tag{1}$$

$$with S(x) = \begin{cases} 1 & |x| \geq T_{LBP} \\ 0 & |x| < T_{LBP} \end{cases}$$

Where n_c be magnitude of middle pixel (x_c, y_c), n_p be the intensity of adjacent pixels with p locates radius on a circle with R , n_c is the middle pixel while $T_{LBP} > 0$ is a small positive threshold for image regions is the approach provides robustness for flat levels [19]. The locations of n_p (neighboring pixels) for $R=1$ and $P=8$. Commonly, the points of n_p are not visible for center image pixels. Hence bilinear interpolation determines the intensity of n_p . An LBP pixels rotation can be achieved by performing the circular bitwise right shift values minimizes and simplifies as a binary number. In some cases, a group of unique pattern decreases to 36. A pattern is constantly unique in circular, but sequence of bits consists only for more than two transitions like 0 with 1 or 1 with 0. The non-uniform patterns concerns all patterns as individual pattern. Further, a group of unique patterns decreases to 10 (8-bit LBP) i.e., 9 uniform patterns consider for grouping a category of non-unique patterns. The unique pattern displays neighboring pixels with blue colour, if the middle pixel is greater than T_{LBP} specifies intensity difference along these couple of bits which are least than T_{LBP} is triggered, if not remaining

region is coloured by red.

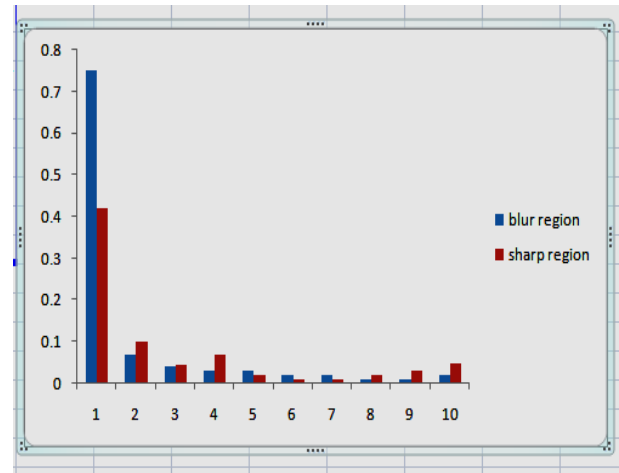


Fig. 2. Histogram of LBP patterns.

The histogram of nine LBP uniform patterns displays blurred and sharp regions selects alternatively a hundred images from the available dataset of 700 partial blurred images along these ground truth images specifies blurred and sharp regions. Along these Bin 9 provides the number of non-uniform patterns that displays the frequencies of 6, 7, 8, 9 signify the blurred regions which are less than that of sharp regions. It means that in smoother areas, most neighbouring pixels will have the same intensity denotes with n_c but in some cases, only a few neighbouring regions triggers with less value makes lower uniform patterns but only fewer triggered neighbors will be more probable. Sharpness metric considers following observations:

$$m_{LBP} = \frac{1}{N} \sum_{i=6}^9 n(LBP_{8,1}^{riu2i}) \tag{2}$$

Here $n(LBP_{8,1}^{riu2i})$ is 8-bit LBP specification indicates the no. of rotations of uniform patterns and N specifies total number of pixels from chosen local region normalizes the metric by $m_{LBP} \in [0, 1]$. Measuring roughness in the LBP domain is an advantage over LBP features are robust but illumination changes occur always in natural images. The threshold T_{LBP} controls the proposed metric's effects on roughness. The extending T_{LBP} , provides a less sensitive metric for obtaining roughness determines in two terms i.e., roughness sensitivity as well as noise robustness. In some cases, high sensitivity sharpness needs noise reduction filter employs as non-local means. Different metric response obtaining distinct levels of obscure as ($T_{LBP}=0.016$) as well as sharpness ranges in between $\sigma = 0.2, 1.0$ these values. In some cases, the intersection response value ranges for rough and obscure regions will be still smaller than other metrics. Thus, simple thresholding facilitates the segmentation of blurred smooth and sharp region all these compare with

different measurements. At last, metric response reduce the levels of blur determine regions with more exactness and consistency. The histogram of LBP patterns for distinct spots are sampled with transitive, sharp and blurred regions. Whereas in ground truth images white color denotes the sharp regions, black color denotes the blurred region all these refers threshold values of M_{LBP} , T_{LBP} .

IV. PROPOSED WORK

This section describes about our algorithm for segmenting blurred and rough regions that specify LBP sharpness metrics. Additionally KNN metrics is added with LBP metrics. Thus algorithm can be summarized in five main steps : Multi-Scale Sharpness Map, Alpha Matting Initialization, computation of Alpha map, Multi-scale Inference and extracts LBP with KNN.

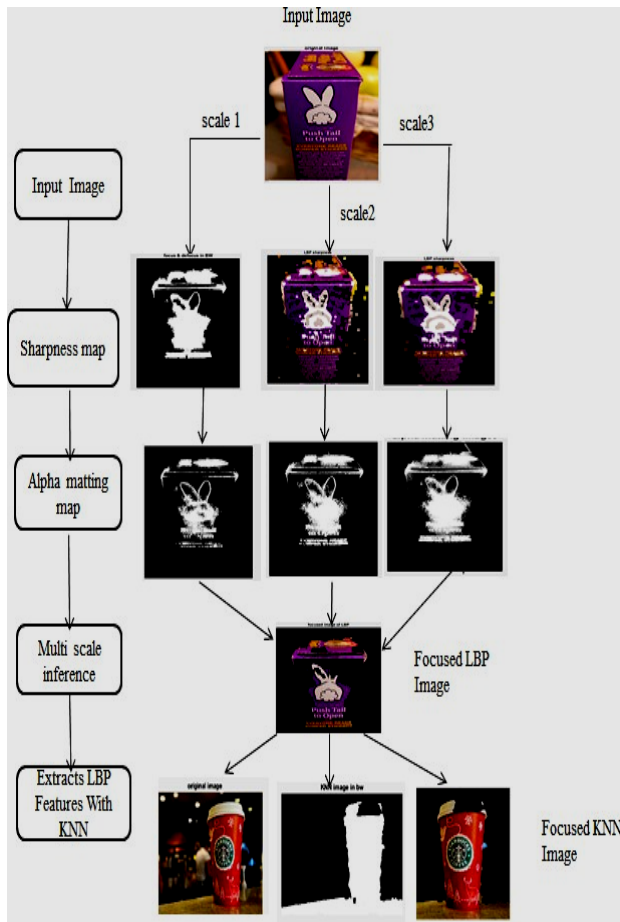


Fig. 3. Blur segmentation algorithm

A. Multi Scale Roughness Map:

In this Multi scale, Sharpness map is considered using m_{LBP} ; The metrics of sharpness consider each image pixel as a local patch all these roughness maps construct with 3

scales specifies with local patch size. Beside the Sharpness, maps computes constant time for each pixel represents by P, R.

B. Alpha Matting Initialization:

It is a process of splitting an image into background and forward regions. It can be expressed as follows:

$$I(x, y) = \alpha_{x,y} F(x, y) + (1 - \alpha_{x,y})B(x, y) \quad (3)$$

From Equation (3) $\alpha_{x,y}$ be the blur value on pixel position (x,y) determines a pixel as a foreground. Usually alpha matting is necessary to know the foreground and background pixels, by initiating those pixels with $\alpha=1$, $\alpha=0$ consequently, illustrates background as "blurred" and foreground as "sharp" regions, by initiating alpha matting process automatically applies double times threshold to sharpness maps computes an initial value of α for each pixel:

$$mask^s(x, y) = \begin{cases} 1, & \text{if } m_{LBP}(x, y) > T_{m1} \\ 0, & \text{if } m_{LBP}(x, y) > T_{m1} \\ m_{LBP}(x, y), & \text{otherwise} \end{cases} \quad (4)$$

Here s indicates scale, and masks (x, y) is the initial α map for sth scale.

C. Computation of Alpha Map:

Levin proposed α -map is for minimizing the cost Function:

$$E(\alpha) = \alpha^T L_{\alpha} + \lambda(\alpha - \hat{\alpha})(\alpha - \hat{\alpha})^T \quad (5)$$

Here α signifies a vectorized α - map, $\hat{\alpha}$ specifies vectorized alpha map from the above step, L indicates matting of Laplacian matrix. Usually first component specifies the smoothness term and second component is similar to data fitting $\hat{\alpha}$ [30]. By applying alpha matting at each scale shown in fig 10. Finally, figure specifies alpha map at each scale as $4 \alpha^s$, s = 1, 2, 3.

D. Multi Scale-Inference:

Alpha map computes on 3 different scales describes regarding graphical multi-scale displays a final image. The overall energy on the graphic Model is defined as follows:

$$E(h) = \sum_{s=1}^3 \sum_t |h_i^s - \hat{h}_i^s| + \beta \left(\sum_{s=1}^3 \sum_i \sum_{j \in \mathcal{N}(i)} |h_i^s - \hat{h}_j^s| \sum_{s=1}^2 \sum_t |h_i^s - h_j^{s+1}| \right) \quad (6)$$

Where $h_i^s = \alpha_i^s$ is the alpha map for S scale as per

earlier step, h_i^s specifies sharpness. First Term in RHS is Unary term and is the cost for specifying for sharpness value and second term specifies Pairwise term represents smoothness for distinct and similar scales. Weight of β provides the necessity of 2 terms performs loopy propagation. The final output of the algorithm indicates sharpness map represents the largest scale, where grayscale image with higher intensity specifies greater sharpness.

E. Extracts LBP with KNN:

In this step image will be implemented first then extracts LBP features with KNN. At last KNN image is displayed also calculates precision and recall values.

F. Precision and Recall:

Usually Recall and Precision values initiate for all algorithms segments final sharpness maps with different threshold values:

$$precision = \frac{R \cap R_g}{R}, recall = \frac{R \cap R_g}{R_g} \tag{7}$$

Where R be set of pixels for segmented obscured region and R_g be set of pixels for ground truth blurred region. When comparing precision and recall values for both LBP and KNN evaluates less time based on the image.

V. RESULTS

In this, the selected image displays as it is, but the only object is focused, and the other part is defocused with black and white colors. The white color denotes focused region and black color denotes the defocused region.



Fig. 4. (a) Input Image (b) Focus as well as Defocus Image.

The image displays with multi scale-sharpness using 3 different scales. In each scale, the process is distinct from one other, but each image pixel computes its local patch with local size. All these sharpness maps estimate per pixel with constant time for P and R parameters.



Fig. 5. LBP roughness at scale 1 and scale 2.

After dividing the image into three scales, the alpha matting method is initialized for the selected image. It defines for decomposing an image into a foreground and background. The foreground and background regions are referred as a sharp regions and as the blur regions.

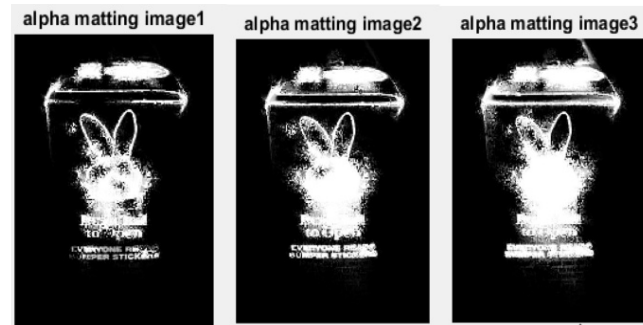


Fig. 6. Alpha matting images at scale 1, scale 2, scale 3 respectively.

In this, all steps processes, at last altogether display a focused LBP image. However, a blur in background region is determined as blur part is colored with black color and the sharp region in the foreground region is colored with white color is because of using the alpha method. Thus by using the alpha method, the image is processed in a single image in terms of three scales, at last, a focused LBP image is displayed.

Focused Image of LBP



Fig. 7. Focused image for LBP.

Basically, the image is selected based on splitting of image in the foreground and background parts extracts using nearest neighbors features displays with focus and defocus regions.

Original Image



KNN Image in BW



Fig. 8. KNN image in BW.

In this step, the selected image is displayed as it is, in the overall image the only focused object is visible remaining blur part can't be seen. Based on the image which is nearer to the selected pixel or k-value, the only majority of neighbor pixels are displayed.

KNN Image



Fig. 9. KNN image.

VI. CONCLUSION

Defocus blur segmentation proposes simple LBP roughness metric along with KNN metrics. KNN depends on LBP patterns which specify focus and defocus image regions. Segmentation method on sharpness metrics based on sparse representation measures the multi scale inference framework. Basically algorithms performance is maintained automatically by selecting the threshold value. Our roughness metric measures group of LBP patterns along with nearest neighbor regions combines real time matting algorithms over KNN segmentation algorithm which has significant speed as an advantage. The proposed segmentation algorithm for defocus blur and roughness metrics on Local Binary Patterns exploits the observation upon majority of local images. Considerably native binary patterns have low bounds for comparing patches in obscured regions with other rough regions. Along these, image matting and multi scale inference, have a tendency to obtain high quality sharpness maps. These results show that our proposed method for defocus blur gives better results when compared to the state-of-art existing techniques.

REFERENCES

- [1] R. Ferzli and L. J. Karam, A no-reference objective image sharpness metric based on the notion of just noticeable blur (JNB), *IEEE Trans. Image Process.*, vol. 18, no. 4, pp. 717-728, Apr. 2009.
- [2] P. Marziliano, F. Dufaux, S. Winkler, and T. Ebrahimi, A no-reference perceptual blur metric, in *Proc. Int. Conf. Image*

- Process., vol. 3, 2002, pp. III-57- III- 60.
- [3] N. D. Narvekar and L. J. Karam, A no-reference image blur metric based on the cumulative probability of blur detection (CPBD), IEEE Trans. Image Process., vol. 20, no. 9, pp. 2678-2683, Sep. 2011.
- [4] R. Hassen, Z. Wang, and M. M. A. Salama, Image sharpness assessment based on local phase coherence, IEEE Trans. Image Process., vol. 22, no. 7, pp. 2798-2810, Jul. 2013.
- [5] T. Thongkamwitoon, H. Muammar, and P.-L. Dragotti, An image recapture detection algorithm based on learning dictionaries of edge profiles, IEEE Trans. Inf. Forensics Security, vol. 10, no. 5, pp. 953-968, May 2015.
- [6] S. Bae and F. Durand, Defocus magnification, Comput. Graph. Forum, vol. 26, no. 3, pp. 571-579, 2007.
- [7] S. Zhuo and T. Sim, Defocus map estimation from a single image, Pattern Recognit., vol. 44, no. 9, pp. 1852-1858, 2011.
- [8] C. Kim, Segmenting a low-depth-of-field image using morphological filters and region merging, IEEE Trans. Image Process., vol. 14, no. 10, pp. 1503-1511, Oct. 2005.
- [9] J. Z. Wang, J. Li, R. M. Gray, and G. Wiederhold, Unsupervised multiresolution segmentation for images with low depth of field, IEEE Trans. Pattern Anal. Mach. Intell., vol. 23, no. 1, pp. 85-90, Jan. 2001.
- [10] C. S. Won, K. Pyun, and R. M. Gray, Automatic object segmentation in images with low depth of field, in Proc. Int. Conf. Image Process., vol.3. Jun. 2002, pp 805-808.
- [11] X. Zhu, Measuring spatially varying blur and its application in digital image restoration, Ph.D. dissertation, Dept. Elect. Eng., Univ. California, Santa Cruz, CA, USA2013.
- [12] J. Shi, L. Xu, and J. Jia, Discriminative blur detection features, in Proc. IEEE Conf. Comput. Vis. Pattern Recognit. (CVPR), Jun. 2014, pp. 2965-2972.
- [13] B. Su, S. Lu, and C. L. Tan, Blurred image region detection and classification, in Proc. 19th ACM Int. Conf. Multimedia, 2011, pp.1397-1400.
- [14] C. T. Vu, T. D. Phan, and D. M. Chandler, S3: A spectral and spatial measure of local perceived sharpness in natural images, IEEE Trans. Image Process., vol. 21, no.3, pp. 934-945, Mar. 2012
- [15] J. Shi, L. Xu, and J. Jia, Just noticeable defocus blur detection and estimation, in Proc. IEEE Conf. Comput. Vis. Pattern Recognit. (CVPR), Jun. 2015, pp. 657-665.
- [16] S. Zhuo and T. Sim, Defocus map estimation from a single image, Pattern Recognit., vol. 44, no. 9, pp. 1852-1858, 2011.
- [17] A. Levin, D. Lischinski, and Y. Weiss, A closed-form solution to natural image matting, IEEE Trans. Pattern Anal. Mach. Intell., vol. 30, no. 2, pp. 228-242, Feb2008.
- [18] X. Zhu, S. Cohen, S. Schiller, and P. Milanfar, Estimating spatially varying defocus blur from a single image, IEEE Trans. Image Process., vol. 22, no. 12, pp. 4879-4891, Dec. 2013.
- [19] A. Levin, Y. Weiss, F. Durand, and W. T. Freeman, Understanding and evaluating blind deconvolution algorithms, in Proc. IEEE Conf. Comput. Vis. Pattern Recognit. (CVPR), Jun. 2009, pp. 1964-1971.
- [20] A. Chakrabarti, T. Zickler, and W. T. Freeman, Analyzing spatially-varying blur, in Proc. IEEE Conf. Comput. Vis. Pattern Recognit. (CVPR), Jun. 2010, pp. 2512-2519.